ACS NANO

www.acsnano.org

ARTICLE

Laser Writing Block Copolymer Self-Assembly on Graphene Light-Absorbing Layer

Hyeong Min Jin,[†,⊥] Seung Hyun Lee,[‡,⊥] Ju Young Kim,[†] Seung-Woo Son,[§] Bong Hoon Kim,[†] Hwan Keon Lee,[‡] Jeong Ho Mun,[†] Seung Keun Cha,[†] Jun Soo Kim,[†] Paul F. Nealey,[∥] Keon Jae Lee,[*,‡] and Sang Ouk Kim[*,†]

[†]National Creative Research Initiative Center for Multi-Dimensional Directed Nanoscale Assembly, Department of Materials Science and Engineering, KAIST, Daejeon 34141, Republic of Korea

[‡]Department of Materials Science and Engineering, KAIST, Daejeon 34141, Republic of Korea

[§]Department of Applied Physics, Hanyang University, Ansan, Gyeonggi-do 15588, Republic of Korea

[∥] Institute for Molecular Engineering, University of Chicago, Chicago, Illinois 60637, United States

Supporting Information

ABSTRACT: **Recent advance of high-power laser processing allows for rapid, continuous, area-selective material fabrication, typically represented by laser crystallization of silicon or oxides for display applications. Two-dimensional materials such as graphene exhibit remarkable physical properties and are under intensive development for the manufacture of flexible devices. Here we demonstrate an area-selective ultrafast nanofabrication method using low intensity infrared or visible laser irradiation to direct the self-assembly of block copolymer films into highly ordered manufacturing-relevant architectures at the scale below 12 nm. The fundamental principles underlying this light-induced nanofabrication mechanism include the self-assembly of block copolymers to proceed across the disorder−order transition under large thermal gradients, and the use of chemically modified graphene films as a flexible and conformal light-absorbing layers for transparent, nonplanar, and mechanically flexible surfaces.**

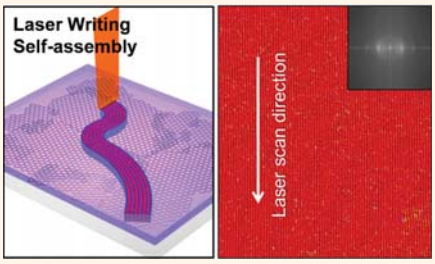

KEYWORDS: *block copolymer, self-assembly, directed self-assembly, laser, graphene, photothermal effect*

Molecular self-assembly is generally driven by thermal fluctuations as the structural system evolves toward thermodynamic minima.[1,2] For self-assembly of macromolecular systems,[3−5] development of processes with high chain mobility is critical to approach the equilibrium state in an application-relevant time scale. Typically, annealing at high temperature[6−13] or in the presence of solvent[14−19] promotes the mobility of polymer chains during processing. Unfortunately, limits on high temperature treatment are imposed by thermal degradation of organic polymeric molecules, even under inert atmosphere, and the use of solvents introduces complexity in terms of the propensity to form nonequilibrium structures during solvent evaporation and challenges in the integration with existing manufacturing processes.

Laser processing is an emerging material fabrication method relying on localized surface photothermal reaction and is highly motivated from the enormous advantages, such as rapid continuous processability, area selectivity, and minimal influence on the neighboring structures.[20] High energy laser photothermal processes with excimer laser [XeCl, wavelength (λ) = 308 nm] are well established for the area-selective crystallization of silicon and other inorganic materials.[21−24] Controlled instantaneous irradiation by laser beams enables effective phase transformations of the inorganic materials at highly confined desired locations. Suitability for continuous processing makes this approach attractive for the manufacture of flexible devices. Motivated by the unique advantages, laser processing has been also introduced for organic materials, such as chemically amplified resists,[25−28] polymer direct patterning,[29,30] and molecular self-assembly.[31−38] Among them, directed self-assembly of block copolymer (BCP) using laser has exploited the extremely high thermal gradient from focused laser photothermal effect.[32−37] Cold zone annealing (CZA) mechanism is predominantly employed, whose maximum photothermal heating temperature is below order−disorder transition temperature (T_{ODT}) of BCPs. Accordingly, the ordering of self-assembled nanodomains occurs *via* defect kinetics and reveals relatively low degree of ordering. For the further enhancement of nanodomain ordering, additional

Received: November 28, 2015
Accepted: February 12, 2016
Published: February 12, 2016

DOI: 10.1021/acsnano.5b07511
ACS Nano 2016, 10, 3435−3442

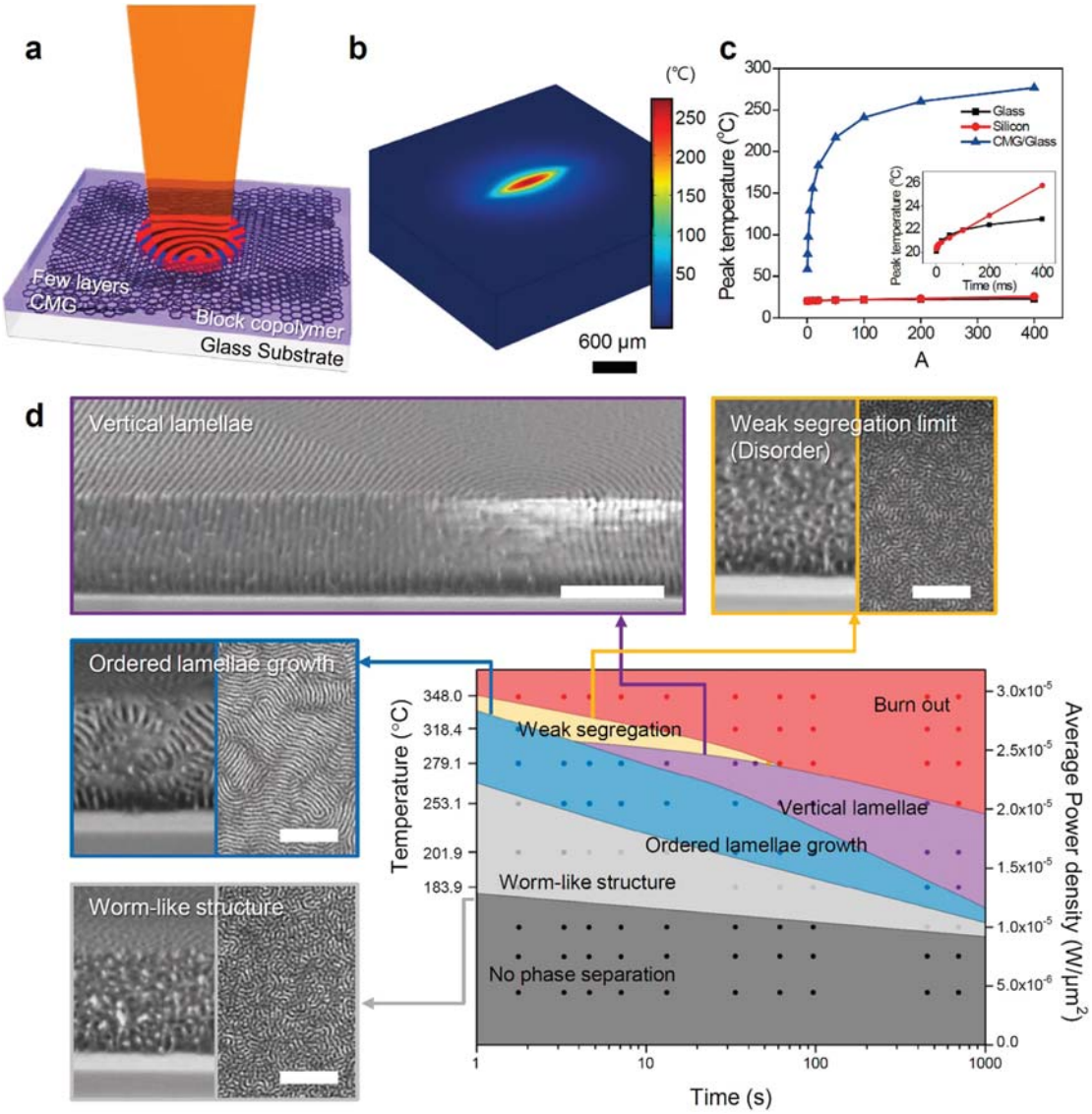

Figure 1. BCP self-assembly under static laser photothermal treatment. (a) Schematic illustration of area-selective BCP self-assembly with static laser irradiation on CMG/glass substrate. (b) FEM analysis of the in-plane temperature profile on CMG/glass surface by focused elliptic laser irradiation. (c) Time evolution of peak temperature on bare glass, bare silicon and CMG/glass surfaces by laser irradiation (average power density = 2.33×10^{-5} W/μm^2). Inset shows a zoom-in of the peak temperature variation of bare glass and bare silicon surfaces. (d) Morphology evolution in BCP thick films on CMG (transmittance = 89.2%) with average laser power density and irradiation time. Along with the increase of power density and irradiation time, BCP morphology sequentially evolves through no phase separation (disorder), worm-like structure, ordered lamellae growth, vertical lamellae, weak segregation and finally burn out. Scale bar: 600 μm (b), 300 nm (d).

ordering method such as solvent mediation[33] and photothermal shearing[34−37] have been supplemented.

In this work, we demonstrate that low energy laser photothermal treatment exploiting graphene-based light-absorbing layer is an effective and versatile route to promote chain mobility for polymer self-assembly. Significantly, we show that the process is amenable for use with flexible and three-dimensional complex substrates. For the self-assembly of polymer molecules, we use low energy lasers with visible or infrared wavelength range to avoid radiation damage of the organic materials.[38,39] The laser irradiation is used in conjunction with graphene-based thin films. Few-layer chemically modified graphene (CMG) plays the essential role of locally converting the low energy radiation to thermal energy.[40] The CMG's superior mechanical properties enable conformal coating and processing on planar and nonplanar substrates.[41−44] Direct irradiation of the focused laser beam onto a BCP thin-film coated on a graphene layer successfully induces equilibrium self-assembled morphologies with controlled orientation of nanodomains such as vertical cylinders and lamellae. Owing to the localized rapid photothermal heating/quenching, processing in inert atmosphere is not required, and the BCP film does not show any reflow even at the surface of flexible or 3D complex substrates. Above all, directional self-assembly after complete melting arising from lateral scanning of the focused laser beam results in the vertically oriented domains with exceptionally high degrees of long-range order in the plane

DOI: 10.1021/acsnano.5b07511
ACS Nano 2016, 10, 3435−3442

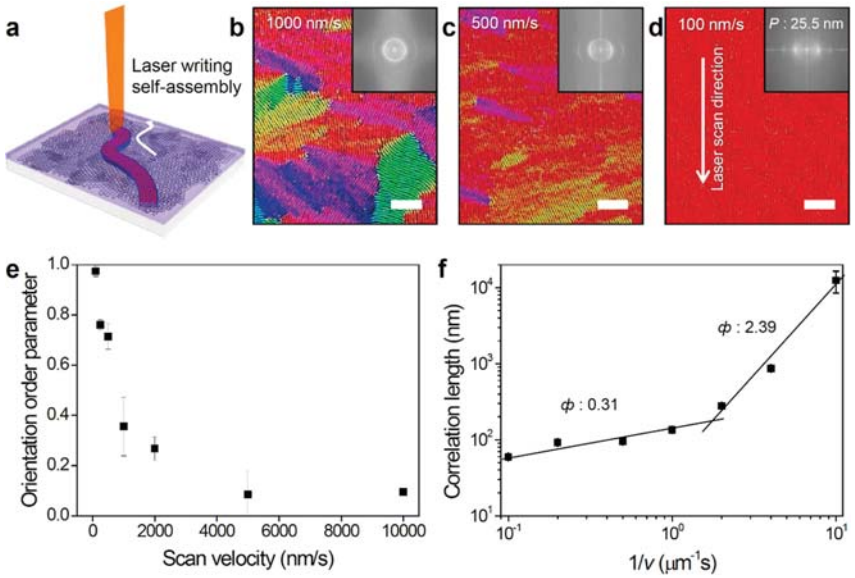

Figure 2. Laser writing BCP self-assembly. (a) Schematic illustration of highly oriented BCP assembly by lateral laser scanning. Orientation color maps for lamellar BCP morphologies obtained at different lateral laser scanning velocities (v) (b) 1000, (c) 500, and (d) 100 nm/s with the power density of 2.33 × 10^{-5} W/μm^2. The inset figures in each image are Fast Fourier transform (FFT) results. (e) Orientation ordering parameter (Ψ) vs v and (f) correlation length vs 1/v. Scale bar: 300 nm (b–d).

of the film, a prerequisite for many applications in nanomanufacturing.

RESULTS AND DISCUSSION

Figure 1a presents the BCP self-assembly under static laser photothermal treatment. We use a focused pulsed near-IR laser beam (ytterbium pulsed fiber laser, wavelength (λ) = 1064 nm, pulse frequency = 300 kHz, pulse duration = 200 ns) with low laser power density (typical average power density of ~2.33 × 10^{-5} W/μm^2). Direct laser irradiation onto the solution-cast (disordered) BCP films on typical substrates, such as bare glass or silicon substrate, does not induce a sufficient photothermal heating effect due to the low photoabsorbance or high thermal conductivity of the substrate materials (Supporting Information text and Figures S1 and S2 and Table S1) to anneal the BCP. In this regard, a graphene-based light absorption layer is essential for effective photothermal conversion due to its strong broadband absorption (2.3%/layer).[40] Graphene is also an attractive material because it may serve as a flexible substrate, with mechanical flexibility, easy transferability, and van der Waals force-mediated universal adhesion.[43] We use solution casting of graphene oxide (GO) and subsequent thermal/chemical reduction to prepare CMG[45−47] light-absorbing layers on many different substrate materials, including transparent, flexible, and nonplanar substrates.

Finite element method (FEM) analysis of the pulsed near IR laser absorption (λ = 1064 nm, average power density = 2.33 × 10^{-5} W/μm^2) of CMG (transparency = 89.2%, thickness = ~2 nm)/glass substrate for elliptical radiation area (d_x = 600 μm, d_y = 100 μm) is shown in Figure 1b. Supported by the simulation data, the surface temperature of the CMG reaches ~280 °C (ΔT_{CMG} = 256.71 K) at the center of irradiated region after 400 ms pulsed laser heating (Figures 1c and S3–S6). Owing to the superior light absorption of CMG, only four layers of CMG enable ~90 times higher temperature increase than bare glass (ΔT_{Glass} = 2.9 K) for the same laser dose (Figure 1c). Notably, extremely large thermal gradients, ∇T_{max} (*ca.* 1.35 K/μm), hard to obtain by conventional thermal heating, are also realized by the highly confined instantaneous photothermal conversion (Figure S7) (see also Supporting Information).

Figure 1d demonstrates the morphology evolution in a 300 nm thick lamellar BCP film (PS-*b*-PMMA, M_n of PS and PMMA blocks = 25 and 26 kg mol^{-1}, respectively) blended with short neutral random copolymer chains (PS-*r*-PMMA, M_n = 17 kg mol^{-1}), (7:3 weight ratio). The short neutral random copolymer chains greatly enhance the structural defect annihilation and thus facilitate highly ordered self-assembled structure formation.[48] Short neutral chains play two principal roles in BCP thin films during laser directed self-assembly. (1) Effective enhancement of BCP chain mobility for highly ordered self-assembled structure from excess free volume, (2) reduction of T_{ODT} (~reduction of effective χN) to reach the order to disorder transition at moderate temperature. At a weak laser power density below 1.0 × 10^{-5} W/μm^2, disordered or worm-like structure is formed regardless of irradiation time (dark and light gray zone). At a higher power density, the BCP film begins to form ordered lamellar structure (blue zone) but lamellar domains are randomly oriented in the film thickness direction as well as in the plane of the film. A further increase of the laser power density or irradiation time (typically 2.33 × 10^{-5} W/μm^2 for 10 s) results in the formation of a vertically oriented lamellar morphology over the entire film thickness. In our typical setup using an ellipsoid-shaped laser beam (d_x = 600 μm, d_y = 100 μm), vertical lamellae are obtained over a broad center area of the elliptic region (d_x = 300 μm, d_y = 40 μm), where temperature is higher than 260 °C (purple zone). Importantly, the CMG layer has identical interfacial energies for PS and PMMA blocks of the copolymer to facilitate the surface vertical lamellar alignment of PS-*b*-PMMA as a thermodynamic equilibrium condition.[46] As the laser power density is further increased up to 2.70 × 10^{-5} W/μm^2, morphology transits into a disordered state near the order–disorder transition (yellow zone). Excessive power density over 2.92 × 10^{-5} W/μm^2 causes thermal degradation of the organic BCP films (red zone). The

DOI: 10.1021/acsnano.5b07511
ACS Nano 2016, 10, 3435–3442

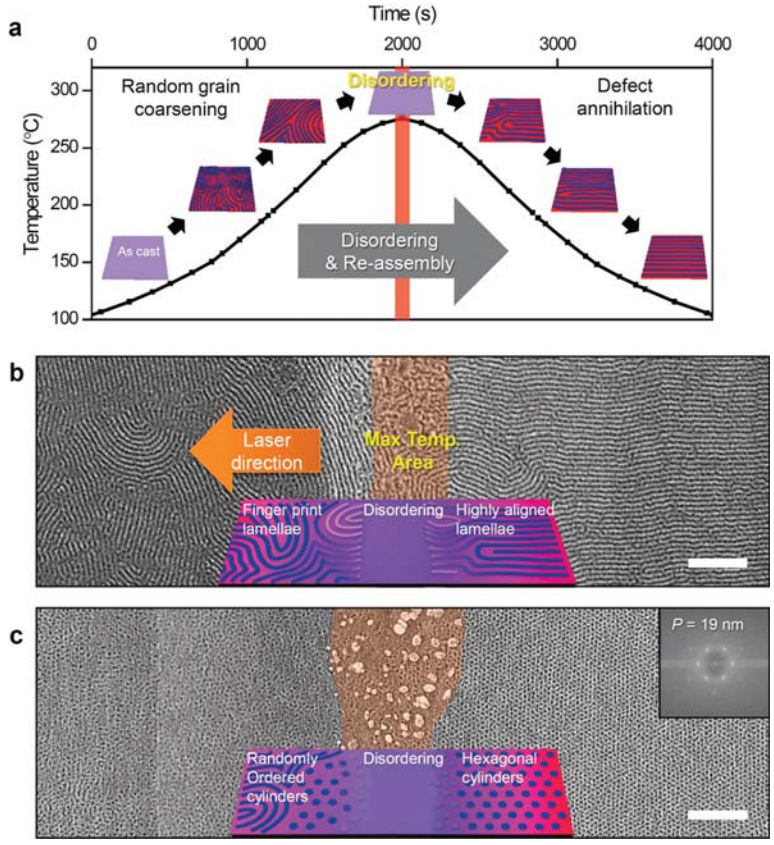

Figure 3. Mechanism for spontaneous BCP nanodomain alignment by laser scanning. (a) Simulated temperature profile in BCP film plane during lateral laser scanning (v = 100 nm/s). Insets show schematic illustrations for lamellar self-assembled morphology evolution around peak temperature region. (b) SEM image and schematic illustration (inset) for the directional self-assembly of oriented BCP lamellar nanodomains from the disordered melting front (at peak temperature region). (c) SEM image and schematic illustration, FFT (inset) for the formation of large-area single grain of hexagonal vertical cylinder nanodomains from disordered melting front. Scale bar: 300 nm.

uniform and clean BCP film surface indicates no noticeable damage by laser photothermal heating, although the peak power density of the pulsed laser is ~16.7 times higher than average power density at every single pulse (Figure S14).

Lateral scanning of the laser beam in the plane of the BCP film induces spontaneous alignment of nanodomains along the scan direction. Figure 2a schematically illustrates the "laser writing self-assembly". The degree of lamellar alignment is critically dependent upon the laser scan velocity (v). When v > 1000 nm/s, only a weak orientation is observed (Figure 2b). When v < 1000 nm/s, preferred alignment along laser scan direction becomes stronger (Figure 2c), and finally, highly oriented morphology with minimal defects is observed below 250 nm/s (Figure 2d and Figures S8 and S9) (see also Supporting Information). A uniform false color orientation map and sharp dot pattern in Fast Fourier transform (FFT) analysis (Figure 2d, inset) illustrate the high degree of alignment, where the orientation order parameter reaches 0.974 (Figures 2e and S10).

Self-assembled stripe pattern coarsening processes are generally described by

$$\xi(t) \sim t^{\phi} \tag{1}$$

where ξ is correlation length associated with grain size, t is annealing time, and ϕ is growth exponent.[49−51] The ξ can be expressed as a function of v, which is inversely proportional to t

$$\xi(t) \sim \left(\frac{1}{v}\right)^{\phi} \tag{2}$$

We plot the correlation length, ξ as a function of $1/v$ in Figure 2f. When v > 500 nm/s ($1/v$ < 2 μm^{-1} s), a ϕ of 0.31 is obtained, indicating a typical defect annihilation mechanism by defect coupling with a low diffusion barrier.[52] In contrast, a significantly higher value of 2.39 is obtained for v < 500 nm/s. Previous numerical and experimental works have reported that ϕ can be enhanced up to 0.5 under conditions of gradual anisotropic growth[50,53,54] that arise from symmetry breaking perturbation during thermal annealing. Such a large ϕ value of ~2.39 in the low v range signifies that the nanodomain ordering mechanism deviates from the typical anisotropic gradual growth. (Supporting Information text)

The spontaneous nanodomain alignment mechanism upon laser scanning can be directly visualized by SEM (Figure 3). Samples were prepared by abrupt quenching of laser radiation in the middle of the scanning process. According to the intensity profile of the laser beam (Figures 1b and S3), the BCP film undergoes a temperature profile as indicated in Figure 3a. At the front of the scanning beam, the BCP film is exposed to the weak intensity edge of the beam and gradually becomes heated as the beam propagates. Photothermal heating promotes the BCP chain diffusion and triggers microphase separation. Randomly oriented lamellar domains grow and a vertical

DOI: 10.1021/acsnano.5b07511
ACS Nano 2016, 10, 3435−3442

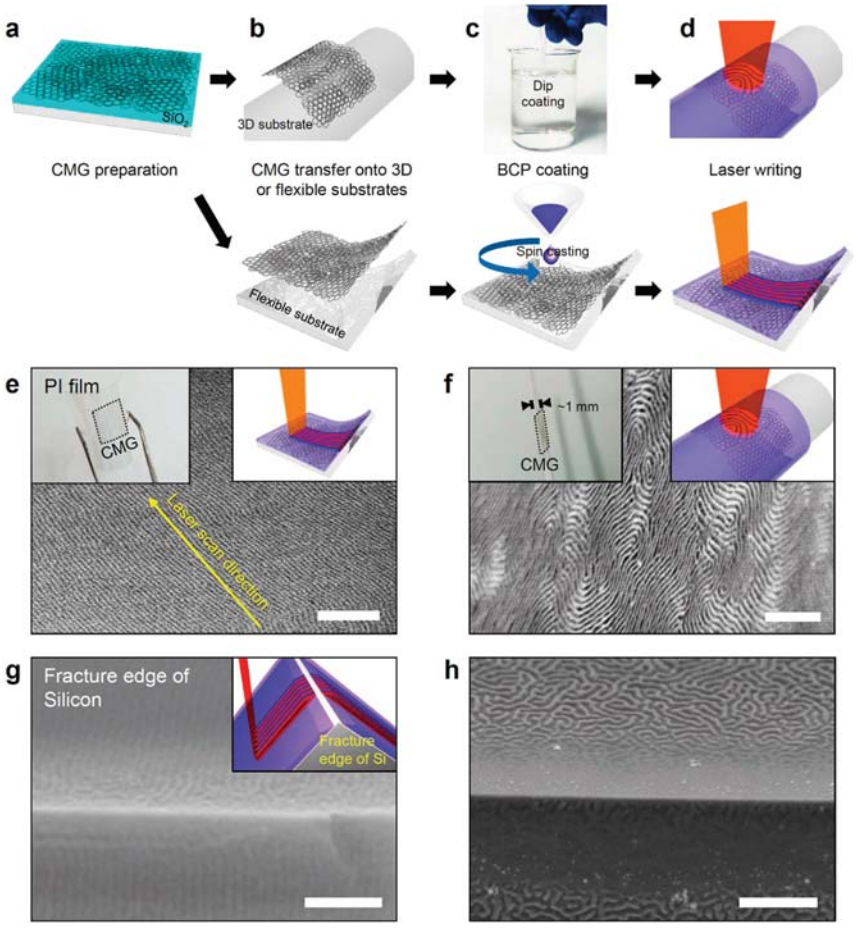

Figure 4. Laser writing BCP self-assembly on flexible or 3D geometry. (a–d) Schematic procedures for laser writing BCP self-assembly on flexible or 3D geometry with conformal CMG light-absorbing layer. (a) CMG film preparation on SiO_2/Si substrate by GO spin-casting and subsequent reduction. (b) CMG film transfer onto 3D or flexible substrates. (c) BCP film casting on CMG coated substrates by dip-coating or spin-casting. (d) Laser scanning on BCP film without geometrical limitation. (e) Aligned BCP lamellar film formed on flexible transparent CMG/polyimide film surface. (f) Lamellar BCP morphology formed on high curvature glass pipet tip surface. (g) Laser writing BCP assembly for aligned lamellae formation and (h) conventional thermal annealing of lamellar film at 90° fractured edge of silicon wafer surface. Scale bar: 600 nm (e, f), 300 nm (h), and 200 nm (g).

lamellar morphology is stabilized. Significantly, when a film area is subject to the center of beam, the temperature exceeds the T_{ODT} and induces a transformation to a disordered phase. In our BCP blends system, 30 wt % short neutral chains significantly lower the χN near 10.495 (χ: Flory–Huggins interaction parameter and N: the degree of polymerization).[55,56] Accordingly, the T_{ODT} is below 300 °C.[48] Further advance of laser beam leads to the downhill temperature profile and the temperature decreases below T_{ODT} again. This triggers the "directional self-assembly"[57−59] from the front of disordered boundary.[60] Notably, without sufficient heating above T_{ODT}, only a weak alignment is observed (typical order parameter <0.1) (Supporting Information text and Figure S11).

Figure 3b shows the SEM image of lamellar BCP films scanned by laser beam at v = 100 nm/s (laser power density = 2.33×10^{-5} W/μm^2). At this low v, the order/disorder boundary can be regarded as a fixed boundary (faster laser scanning is equivalent to homogeneous heating/cooling without the temperature gradient effect). In this quasistatic condition, self-assembled morphology is thermodynamically determined to minimize interfacial area at the order/disorder boundary such that lamellar orientation perpendicular to the order/disorder boundary, that is, parallel to scan direction, is favored.[60] In the following downhill temperature profile, further annealing annihilates the defects and relieves the lamellar modulation and, finally, achieves a highly oriented lamellar morphology. Significantly, in this directional self-assembly, a sharp temperature gradient profile at the order/disorder boundary is crucial for the high degree of ordering. The extremely high ∇T_{max}, over ~1.35 K/μm, is attained by the focused laser beam irradiation coupled with CMG light-absorbing layer enables this high level of alignment (Supporting Information text and Figure S7). We note that this nanodomain alignment mechanism does not require prepatterned substrates[61,62] and can be easily implemented in a continuous manufacturing process, which may significantly broaden the potential applications of self-assembled nanopatterning.

Similar alignment mechanism can be also employed for other BCP systems, including hexagonal vertical cylinders, and surface parallel cylinders. Figure 3c demonstrates the laser writing self-assembly of vertical cylindrical BCPs (PS-*b*-PMMA, M_n of PS and PMMA blocks: 21.5 and 10 kg mol^{-1}, respectively). Owing to the sufficiently small molecular weight of BCPs (~31.5 kg mol^{-1}), the disordered phase could be

DOI: 10.1021/acsnano.5b07511
ACS Nano 2016, 10, 3435–3442

induced without blending short neutral chains. Interestingly, large-area single grain of hexagonal vertically oriented nanocylinders is directly assembled from the disordered front.

Figure 4 presents versatile laser writing self-assembly on flexible substrates or substrates with 3D geometry. Owing to the mechanical flexibility and strong universal adhesion of CMG to arbitrary surfaces, laser writing self-assembly can be implemented on those geometries. CMG films can be transferred onto a desired surface geometry by dry or wet transfer.[47] Facile dip-coating or other solution casting of BCP films is possible on the transferred CMG surface. Chemically inert CMG layer enables direct solution casting of BCP films on conventional polymer surfaces without solvent swelling or damage. Laser photothermal heating induces localized heating of BCP film on CMG layer with minimum thermal effect on the bottom polymer substrate (Figure 4e, inset). Highly ordered nanopatterned morphology is readily attained on such flexible geometries (Figures 4e). In addition, localized and instantaneous laser photothermal heating may induce BCP self-assembly on the high curvature (Radius of curvature: 500 μm) glass pipet surface (Figure 4f) and at the right angled silicon fracture surface (Figure 4g) without noticeable deformation or reflow of BCP thin films, whereas significant deformation is observed with conventional thermal annealing (Figure 4h).

CONCLUSION

Low energy laser photothermal process successfully addresses the longstanding challenges of self-assembly-based nanopatterning, that is, area-selective patternability (Figure S12), for flexible and 3D geometry and nanodomain orientation control without surface prepattered structures. Parallel scanning with slit beams or beam arrays can be also implemented for the large-area continuous processing of nanostructures with desired orientations. This low energy laser process with minimal beam damage, synergistically combined with flexible and conformal CMG photothermal conversion layer, opens up the unexplored potential of laser processing for organic and organic−inorganic hybrid materials toward thermodynamically stable 3D and flexible structures.

METHODS

Materials. Block copolymers (BCPs) were purchased from Polymer Source Inc. Short random copolymers were synthesized by nitroxide-mediated living radical polymerization.[63,64] Graphite powder and toluene (99.8%, anhydrous) were purchased from Sigma-Aldrich. Sulfuric acid, hydrochloric acid (HCl, 97%), potassium permanganate, hydrogen peroxide (H_2O_2, 30%), and isopropyl alcohol (C_3H_8O, 99.5%) were purchased from Junsei Chemical Co., Ltd. Hydrofluoric acid (HF, ACS reagent, 48−51%) was purchased from J.T. Baker. Transparent polyimide film (Neopulim L-3450) was purchased from Mitsubishi Gas Chemical, Inc. Ruthenium tetroxide staining agent was purchased from Electron Microscopy Sciences.

Preparation of Graphene Oxide (GO) Solution. Graphene oxide (GO) was prepared from natural graphite powders by a modified Hummer's method.[65,66] Natural graphite (1 g, Sigma-Aldrich) was mixed with 40 mL of concentrated sulfuric acid in the presence of 3.5 g of potassium permanganate for 2 h. After sufficient oxygenation, excess amount of water and 30% of hydrogen peroxide (H_2O_2) were added in the mixture. Then, GO was separated by vacuum filtration. The obtained graphite oxide powder (~2 g) was filter-washed with 1 M hydrochloric acid (HCl) solution and deionized (DI) water and dispersed in 1 L of DI water again. Graphite oxide was exfoliated into monolayer flakes by sonication for 1 h. Unexfoliated flakes were removed by centrifugation at 18 000 rpm. The resultant monolayer GO aqueous dispersion was sealed in a dialysis membrane (Spectra/Por Dialysis Membrane MWCO: 6−8000) and sunk in DI water for 3 weeks. The DI water was exchanged every day. Suitable concentration of GO solution for spin-casting was achieved by adding additional water.

Preparation of CMG Substrate and BCP Thin Films. For the formation of CMG layer, multilayer GO film was spin-cast with gentle N_2 gas blowing at various mother substrates, such as quartz glass and SiO_2/Si substrate. The thickness of GO film was controlled by concentration of GO solution and RPM of spin-casting. GO thin film was chemically modified for a suitable surface energy by the following two methods. (i) Thermal treatment (700 °C, 1 h) under H_2 gas atmosphere or (ii) chemical treatment under hydrazine monohydrate vapor for 1 h. For nonplanar substrates, CMG thin film was transferred from CMG/SiO_2 wafer by hydrofluoric-acid-assisted wet transfer.[47,67]

A lamellar forming PS-*b*-PMMA copolymer, whose number-average molecular weight (M_n) of PS and PMMA blocks are 25 and 26 kg mol^{-1}, respectively, was blended with short chain neutral PS-*r*-PMMA random copolymer (M_n = 17 kg mol^{-1}) (7:3 weight ratio). Cylinder forming PS-*b*-PMMA copolymers, whose M_n of PS and PMMA blocks are 21.5 and 10 kg mol^{-1}, respectively, were used in this study. BCP films are spin-cast from toluene solutions with a BCP concentration in 2−8 wt % for the precise thickness control. Upon planar substrates, BCP thin films were directly spin-cast, whereas BCP thin films were dip-coated on nonplanar substrates. Upon Si fracture edge, CMG layer overlaid with spin-cast BCP thin film was directly transferred by wet transfer method.[47,67]

Laser Writing BCP Assembly. Focused laser beam (λ = 532 nm, 1064 nm) was directly irradiated onto BCP thin film overlaid upon laser absorbing CMG layer. In the case of near IR laser, low-duty cycle of pulsed IR laser (pulse frequency = 300 kHz and pulse duration = 200 ns) was used for moderate photothermal treatment. The beam has an elliptic shape (d_x = 600 μm, d_y = 100 μm) with the power density between 0 and 10^{-4} W/μm^2. Entire laser process was successfully carried out in ambient condition owing to the ultrafast laser photothermal process. For the lateral laser scanning with controlled scan rates from 100 nm/s to 1 cm/s and a high-precision $X-Y$ linear moving stage [Stacking of two linear stages, XMS 100 (Newport) and PRO165LM-0400 (Aerotech)] was employed.

ASSOCIATED CONTENT

Supporting Information

The Supporting Information is available free of charge on the ACS Publications website at DOI: 10.1021/acsnano.5b07511.

Calculation of orientation order parameter and correlation length, numerical modeling of laser photothermal conversion, estimate of temperature due to laser irradiation, effect of thermal gradient on domain alignment, morphology evolution of BCP thin films under laser photothermal annealing for various laser power densities and laser scan velocities, laser writing self-assembly below order−disorder transition temperature, morphology evolution of BCP thin films under conventional thermal annealing, and characterization. (PDF)

AUTHOR INFORMATION

Corresponding Authors

*E-mail: keonlee@kaist.ac.kr.

*E-mail: sangouk.kim@kaist.ac.kr.

Author Contributions

$^{\perp}$H.M.J. and S.H.L. contributed equally to this work. S.O.K. proposed the initial idea of this project. H.M.J. was responsible for entire BCP process, preparing the CMG substrate, and SEM and thermal camera characteristics. S.H.L. and H.K.L. were responsible for preparation of laser system, laser writing

DOI: 10.1021/acsnano.5b07511
ACS Nano 2016, 10, 3435−3442

process, and numerical simulation. J.Y.K. was responsible for CMG transfer onto arbitrary substrate and helped the preparation of manuscript. S.W.S. was responsible for the calculation of orientation order, correlation length, and orientation order map. B.H.K. was responsible for the preparation of BCP cross-sectional SEM measurement. J.H.M. helped SEM characterization and the preparation of the manuscript. S.K.C. and J.S.K. were responsible for the additional experiments for the differentiation of weak segregation and thermal degradation morphology. P.F.N. gave an advice for the mechanism of directional self-assembly and joined in the preparation of the manuscript. K.J.L. was responsible for directing laser annealing process and computational analysis. S.O.K. and H.M.J. was responsible for managing all aspects of this project including the writing of manuscript.

Notes

The authors declare no competing financial interest.

ACKNOWLEDGMENTS

This work was supported by the Multi-Dimensional Directed Nanoscale Assembly Creative Research Initiative (CRI) Center (2015R1A3A2033061), and the Hybrid Interface Materials Research Group (Global Frontier Project, 2014M3A6B1075032). S.H.L and K.J.L. were supported by National Research Foundation (NRF) fund of Korea (2014R1A2A1A12067558). P.F.N. acknowledges support from the Department of Energy, Basic Energy Sciences, Materials Science and Engineering Division, Argonne National Laboratory.

ABBREVIATIONS

BCP, block copolymer; CMG, chemically modified graphene; GO, graphene oxide; T_{ODT}, order−disorder phase transition temperature

REFERENCES

(1) Bates, F. S.; Fredrickson, G. H. Block Copolymer Thermodynamics: Theory and Experiment. *Annu. Rev. Phys. Chem.* **1990**, *41*, 525−557.

(2) Whitesides, G. M.; Mathias, J. P.; Seto, C. T. Molecular Self-Assembly and Nanochemistry: A Chemical Strategy for the Synthesis of Nanostructures. *Science* **1991**, *254*, 1312−1319.

(3) Park, M.; Harrison, C.; Chaikin, P. M.; Register, R. A.; Adamson, D. H. Block Copolymer Lithography: Periodic Arrays of ~ 10^{11} Holes in 1 Square Centimeter. *Science* **1997**, *276*, 1401−1404.

(4) Kim, S. O.; Solak, H. H.; Stoykovich, M. P.; Ferrier, N. J.; De Pablo, J. J.; Nealey, P. F. Epitaxial Self-Assembly of Block Copolymers on Lithographically Defined Nanopatterned Substrates. *Nature* **2003**, *424*, 411−414.

(5) Onses, M. S.; Song, C.; Williamson, L.; Sutanto, E.; Ferreira, P. M.; Alleyne, A. G.; Nealey, P. F.; Ahn, H.; Rogers, J. A. Hierarchical Patterns of Three-Dimensional Block-Copolymer Films Formed by Electrohydrodynamic Jet Printing and Self-Assembly. *Nat. Nanotechnol.* **2013**, *8*, 667−675.

(6) Segalman, R. A.; Yokoyama, H.; Kramer, E. J. Graphoepitaxy of Spherical Domain Block Copolymer Films. *Adv. Mater.* **2001**, *13*, 1152−1155.

(7) Cheng, J. Y.; Mayes, A. M.; Ross, C. A. Nanostructure Engineering by Templated Self-Assembly of Block Copolymers. *Nat. Mater.* **2004**, *3*, 823−828.

(8) Stoykovich, M. P.; Muller, M.; Kim, S. O.; Solak, H. H.; Edwards, E. W.; de Pablo, J. J.; Nealey, P. F. Directed Assembly of Block Copolymer Blends into Nonregular Device-Oriented Structures. *Science* **2005**, *308*, 1442−1446.

(9) Bita, I.; Yang, J. K.; Jung, Y. S.; Ross, C. A.; Thomas, E. L.; Berggren, K. K. Graphoepitaxy of Self-Assembled Block Copolymers on Two-Dimensional Periodic Patterned Templates. *Science* **2008**, *321*, 939−943.

(10) Welander, A. M.; Kang, H. M.; Stuen, K. O.; Solak, H. H.; Muller, M.; de Pablo, J. J.; Nealey, P. F. Rapid Directed Assembly of Block Copolymer Films at Elevated Temperatures. *Macromolecules* **2008**, *41*, 2759−2761.

(11) Jo, A.; Joo, W.; Jin, W. H.; Nam, H.; Kim, J. K. Ultrahigh-Density Phase-Change Data Storage without the Use of Heating. *Nat. Nanotechnol.* **2009**, *4*, 727−731.

(12) Felts, J. R.; Onses, M. S.; Rogers, J. A.; King, W. P. Nanometer Scale Alignment of Block-Copolymer Domains by Means of a Scanning Probe Tip. *Adv. Mater.* **2014**, *26*, 2999−3002.

(13) Kim, S.; Nealey, P. F.; Bates, F. S. Directed Assembly of Lamellae Forming Block Copolymer Thin Films near the Order-Disorder Transition. *Nano Lett.* **2014**, *14*, 148−152.

(14) Kim, S. H.; Misner, M. J.; Xu, T.; Kimura, M.; Russell, T. P. Highly Oriented and Ordered Arrays from Block Copolymers *via* Solvent Evaporation. *Adv. Mater.* **2004**, *16*, 226−231.

(15) Tang, C.; Lennon, E. M.; Fredrickson, G. H.; Kramer, E. J.; Hawker, C. J. Evolution of Block Copolymer Lithography to Highly Ordered Square Arrays. *Science* **2008**, *322*, 429−432.

(16) Jung, Y. S.; Ross, C. A. Solvent-Vapor-Induced Tunability of Self-Assembled Block Copolymer Patterns. *Adv. Mater.* **2009**, *21*, 2540−2545.

(17) Park, S.; Lee, D. H.; Xu, J.; Kim, B.; Hong, S. W.; Jeong, U.; Xu, T.; Russell, T. P. Macroscopic 10-Terabit-Per-Square-Inch Arrays from Block Copolymers with Lateral Order. *Science* **2009**, *323*, 1030−1033.

(18) Ross, C. A.; Berggren, K. K.; Cheng, J. Y.; Jung, Y. S.; Chang, J. B. Three-Dimensional Nanofabrication by Block Copolymer Self-Assembly. *Adv. Mater.* **2014**, *26*, 4386−4396.

(19) Kim, J. M.; Kim, Y. J.; Park, W. I.; Hur, Y. H.; Jeong, J. W.; Sim, D. M.; Baek, K. M.; Lee, J. H.; Kim, M. J.; Jung, Y. S. Eliminating the Trade-Off between the Throughput and Pattern Quality of Sub-15 nm Directed Self-Assembly *via* Warm Solvent Annealing. *Adv. Funct. Mater.* **2015**, *25*, 306−315.

(20) Bäuerle, D. W. Overview and Fundamentals. In *Laser processing and chemistry*; Springer: Heidelberg, 2013; pp 3−4.

(21) Im, J. S.; Kim, H. J.; Thompson, M. O. Phase-Transformation Mechanisms Involved in Excimer-Laser Crystallization of Amorphous-Silicon Films. *Appl. Phys. Lett.* **1993**, *63*, 1969−1971.

(22) Sposili, R. S.; Im, J. S. Sequential Lateral Solidification of Thin Silicon Films on SiO_2. *Appl. Phys. Lett.* **1996**, *69*, 2864−2866.

(23) Arora, H.; Du, P.; Tan, K. W.; Hyun, J. K.; Grazul, J.; Xin, H. L.; Muller, D. A.; Thompson, M. O.; Wiesner, U. Block Copolymer Self-Assembly-Directed Single-Crystal Homo- and Heteroepitaxial Nanostructures. *Science* **2010**, *330*, 214−219.

(24) Tan, K. W.; Saba, S. A.; Arora, H.; Thompson, M. O.; Wiesner, U. Colloidal Self-Assembly-Directed Laser-Induced Non-Close-Packed Crystalline Silicon Nanostructure. *ACS Nano* **2011**, *5*, 7960−7966.

(25) Jung, B.; Ober, C. K.; Thompson, M. O.; Chandhok, M. LWR Reduction and Flow of Chemically Amplified Resist Patterns During Sub-Millisecond Heating. *Proc. SPIE* **2011**, *7972*, 79722S.

(26) Jung, B.; Sha, J.; Paredes, F.; Ober, C. K.; Thompson, M. O. Sub-Millisecond Post Exposure Bake of Chemically Amplified Resists by CO_2 Laser Heat Treatment. *Proc. SPIE* **2010**, *7639*, 76390L-76390L−76399.

(27) Singer, J. P.; Kooi, S. E.; Thomas, E. L. Focused Laser Spike (Flask) Annealing of Photoactivated Chemically Amplified Resists for Rapid Hierarchical Patterning. *Nanoscale* **2011**, *3*, 2730−2738.

(28) Jung, B.; Satish, P.; Bunck, D. N.; Dichtel, W. R.; Ober, C. K.; Thompson, M. O. Laser-Induced Sub-Millisecond Heating Reveals Distinct Tertiary Ester Cleavage Reaction Pathways in a Photolithographic Resist Polymer. *ACS Nano* **2014**, *8*, 5746−5756.

(29) Singer, J. P.; Kooi, S. E.; Thomas, E. L. Focused Laser-Induced Marangoni Dewetting for Patterning Polymer Thin Films. *J. Polym. Sci., Part B: Polym. Phys.* **2016**, *54*, 225−236.

DOI: 10.1021/acsnano.5b07511
ACS Nano 2016, 10, 3435−3442

(30) Singer, J. P.; Lin, P. T.; Kooi, S. E.; Kimerling, L. C.; Michel, J.; Thomas, E. L. Direct-Write Thermocapillary Dewetting of Polymer Thin Films by a Laser-Induced Thermal Gradient. *Adv. Mater.* **2013**, *25*, 6100−6105.
(31) Jacobs, A. G.; Liedel, C.; Ober, C. K.; Thompson, M. O. Understanding of PS-*b*-PMMA Phase Segregation under Laser-Induced Millisecond Thermal Annealing. *Proc. SPIE* **2015**, *9423*, 942309.
(32) Jacobs, A. G.; Jung, B.; Ober, C. K.; Thompson, M. O. Control of PS-*b*-PMMA Directed Self-Assembly Registration by Laser Induced Millisecond Thermal Annealing. *Proc. SPIE* **2014**, *9049*, 90492B.
(33) Singer, J. P.; Gotrik, K. W.; Lee, J. H.; Kooi, S. E.; Ross, C. A.; Thomas, E. L. Alignment and Reordering of a Block Copolymer by Solvent-Enhanced Thermal Laser Direct Write. *Polymer* **2014**, *55*, 1875−1882.
(34) Majewski, P. W.; Rahman, A.; Black, C. T.; Yager, K. G. Arbitrary Lattice Symmetries *via* Block Copolymer Nanomeshes. *Nat. Commun.* **2015**, *6*, 7448.
(35) Majewski, P. W.; Yager, K. G. Block Copolymer Response to Photothermal Stress Fields. *Macromolecules* **2015**, *48*, 4591−4598.
(36) Majewski, P. W.; Yager, K. G. Latent Alignment in Pathway-Dependent Ordering of Block Copolymer Thin Films. *Nano Lett.* **2015**, *15*, 5221−5228.
(37) Majewski, P. W.; Yager, K. G. Millisecond Ordering of Block Copolymer Films *via* Photothermal Gradients. *ACS Nano* **2015**, *9*, 3896−3906.
(38) Tan, K. W.; Jung, B.; Werner, J. G.; Rhoades, E. R.; Thompson, M. O.; Wiesner, U. Transient Laser Heating Induced Hierarchical Porous Structures from Block Copolymer-Directed Self-Assembly. *Science* **2015**, *349*, 54−58.
(39) Srinivasan, R. Ablation of Polymers and Biological Tissue by Ultraviolet Lasers. *Science* **1986**, *234*, 559−565.
(40) Nair, R. R.; Blake, P.; Grigorenko, A. N.; Novoselov, K. S.; Booth, T. J.; Stauber, T.; Peres, N. M.; Geim, A. K. Fine Structure Constant Defines Visual Transparency of Graphene. *Science* **2008**, *320*, 1308.
(41) Eda, G.; Fanchini, G.; Chhowalla, M. Large-Area Ultrathin Films of Reduced Graphene Oxide as a Transparent and Flexible Electronic Material. *Nat. Nanotechnol.* **2008**, *3*, 270−274.
(42) Lee, C.; Wei, X.; Kysar, J. W.; Hone, J. Measurement of the Elastic Properties and Intrinsic Strength of Monolayer Graphene. *Science* **2008**, *321*, 385−388.
(43) Geim, A. K. Graphene: Status and Prospects. *Science* **2009**, *324*, 1530−1534.
(44) Kim, K. S.; Zhao, Y.; Jang, H.; Lee, S. Y.; Kim, J. M.; Kim, K. S.; Ahn, J. H.; Kim, P.; Choi, J. Y.; Hong, B. H. Large-Scale Pattern Growth of Graphene Films for Stretchable Transparent Electrodes. *Nature* **2009**, *457*, 706−710.
(45) Park, S.; Ruoff, R. S. Chemical Methods for the Production of Graphenes. *Nat. Nanotechnol.* **2009**, *4*, 217−224.
(46) Kim, B. H.; Kim, J. Y.; Jeong, S. J.; Hwang, J. O.; Lee, D. H.; Shin, D. O.; Choi, S. Y.; Kim, S. O. Surface Energy Modification by Spin-Cast, Large-Area Graphene Film for Block Copolymer Lithography. *ACS Nano* **2010**, *4*, 5464−5470.
(47) Kim, J. Y.; Kim, B. H.; Hwang, J. O.; Jeong, S. J.; Shin, D. O.; Mun, J. H.; Choi, Y. J.; Jin, H. M.; Kim, S. O. Flexible and Transferrable Self-Assembled Nanopatterning on Chemically Modified Graphene. *Adv. Mater.* **2013**, *25*, 1331−1335.
(48) Kim, B. H.; Park, S. J.; Jin, H. M.; Kim, J. Y.; Son, S. W.; Kim, M. H.; Koo, C. M.; Shin, J.; Kim, J. U.; Kim, S. O. Anomalous Rapid Defect Annihilation in Self-Assembled Nanopatterns by Defect Melting. *Nano Lett.* **2015**, *15*, 1190−1196.
(49) Bray, A. J. Theory of Phase-Ordering Kinetics. *Adv. Phys.* **1994**, *43*, 357−459.
(50) Harrison, C.; Adamson, D. H.; Cheng, Z.; Sebastian, J. M.; Sethuraman, S.; Huse, D. A.; Register, R. A.; Chaikin, P. M. Mechanisms of Ordering in Striped Patterns. *Science* **2000**, *290*, 1558−1560.
(51) Boyer, D.; Vinals, J. Domain Coarsening of Stripe Patterns Close to Onset. *Phys. Rev. E: Stat. Phys., Plasmas, Fluids, Relat. Interdiscip. Top.* **2001**, *64*, 050101.
(52) Ruiz, R.; Bosworth, J. K.; Black, C. T. Effect of Structural Anisotropy on the Coarsening Kinetics of Diblock Copolymer Striped Patterns. *Phys. Rev. B: Condens. Matter Mater. Phys.* **2008**, *77*, 054204.
(53) Qian, H.; Mazenko, G. F. Growth of Order in an Anisotropic Swift-Hohenberg Model. *Phys. Rev. E* **2006**, *73*, 036117.
(54) Berry, B. C.; Bosse, A. W.; Douglas, J. F.; Jones, R. L.; Karim, A. Orientational Order in Block Copolymer Films Zone Annealed below the Order-Disorder Transition Temperature. *Nano Lett.* **2007**, *7*, 2789−2794.
(55) Leibler, L. Theory of Microphase Separation in Block Copolymers. *Macromolecules* **1980**, *13*, 1602−1617.
(56) Fredrickson, G. H.; Helfand, E. Fluctuation Effects in the Theory of Microphase Separation in Block Copolymers. *J. Chem. Phys.* **1987**, *87*, 697−705.
(57) De Rosa, C.; Park, C.; Thomas, E. L.; Lotz, B. Microdomain Patterns from Directional Eutectic Solidification and Epitaxy. *Nature* **2000**, *405*, 433−437.
(58) Park, C.; De Rosa, C.; Thomas, E. L. Large Area Orientation of Block Copolymer Microdomains in Thin Films *via* Directional Crystallization of a Solvent. *Macromolecules* **2001**, *34*, 2602−2606.
(59) Angelescu, D. E.; Waller, J. H.; Adamson, D. H.; Register, R. A.; Chaikin, P. M. Enhanced Order of Block Copolymer Cylinders in Single-Layer Films Using a Sweeping Solidification Front. *Adv. Mater.* **2007**, *19*, 2687−2690.
(60) Zhang, H. D.; Zhang, J. W.; Yang, Y. L.; Zhou, X. D. Microphase Separation of Diblock Copolymer Induced by Directional Quenching. *J. Chem. Phys.* **1997**, *106*, 784−792.
(61) Morkved, T. L.; Lu, M.; Urbas, A. M.; Ehrichs, E. E.; Jaeger, H. M.; Mansky, P.; Russell, T. P. Local Control of Microdomain Orientation in Diblock Copolymer Thin Films with Electric Fields. *Science* **1996**, *273*, 931−933.
(62) Angelescu, D. E.; Waller, J. H.; Adamson, D. H.; Deshpande, P.; Chou, S. Y.; Register, R. A.; Chaikin, P. M. Macroscopic Orientation of Block Copolymer Cylinders in Single-Layer Films by Shearing. *Adv. Mater.* **2004**, *16*, 1736−1740.
(63) Hawker, C. J.; Barclay, G. G.; Orellana, A.; Dao, J.; Devonport, W. Initiating Systems for Nitroxide-Mediated "Living" Free Radical Polymerizations: Synthesis and Evaluation. *Macromolecules* **1996**, *29*, 5245−5254.
(64) Mansky, P.; Liu, Y.; Huang, E.; Russell, T. P.; Hawker, C. J. Controlling Polymer-Surface Interactions with Random Copolymer Brushes. *Science* **1997**, *275*, 1458−1460.
(65) Hummers, W. S.; Offeman, R. E. Preparation of Graphitic Oxide. *J. Am. Chem. Soc.* **1958**, *80*, 1339−1339.
(66) Kim, J. E.; Han, T. H.; Lee, S. H.; Kim, J. Y.; Ahn, C. W.; Yun, J. M.; Kim, S. O. Graphene Oxide Liquid Crystals. *Angew. Chem., Int. Ed.* **2011**, *50*, 3043−3047.
(67) Hwang, J. O.; Lee, D. H.; Kim, J. Y.; Han, T. H.; Kim, B. H.; Park, M.; No, K.; Kim, S. O. Vertical ZnO Nanowires/Graphene Hybrids for Transparent and Flexible Field Emission. *J. Mater. Chem.* **2011**, *21*, 3432.

DOI: 10.1021/acsnano.5b07511
ACS Nano 2016, 10, 3435−3442